https://doi.org/10.5194/essd-2022-188
Preprint. Discussion started: 19 July 2022
© Author(s) 2022. CC BY 4.0 License.

Open Access Earth System Science Data Discussions

The PANDA automatic weather station network between the coast and Dome A, East Antarctica

Minghu Ding[1], Xiaowei Zou[1,2], Qizhen Sun[3], Diyi Yang[1], Wenqian Zhang[1], Lingen Bian[1], Changgui Lu[1], Ian Allison[4], Petra Heil[4], Cunde Xiao[5]

[1]State Key Laboratory of Severe Weather, Chinese Academy of Meteorological Sciences, Beijing 100081, China

[2]GNSS research center, Wuhan University, Wuhan 430079, China

[3]Polar Research and Forecasting Division, National Marine Environmental Forecasting Center, Beijing 100081, China

[4]Australian Antarctic Division and Australian Antarctic Program Partnership, University of Tasmania, Australia

[5]State Key Laboratory of Earth Surface Processes and Resource Ecology, Beijing Normal University, Beijing 100875, China

Correspondence to: Minghu Ding (dingminghu@foxmail.com) and Cunde Xiao (cdxiao@bnu.edu.cn)

Abstract: This paper introduces a unique multiyear dataset and the monitoring capability of the PANDA automatic weather station network which includes eleven automatic weather stations (AWS) across Prydz Bay-Amery Ice Shelf-dome area from the coast to the summit of the East Antarctica ice sheet. The ~1460 km transect from Zhongshan to Panda S station follows roughly along ~77° E longitude and covers all geographic and climatic units of East Antarctica. Initial inland observation, near the coast, started in the 1996/1997 austral summer. All AWSs in this network measure air temperature, relative humidity, air pressure, wind speed and wind direction at 1-hour intervals, and some of them can also measure firn temperature and shortwave/longwave radiation. Data are relayed in near real-time via the ARGOS system. Data quality is generally very reliable and the data have been used widely. In this paper, we firstly present a detailed overview of the AWSs, including the sensor characteristics, installation procedure, data quality control protocol, and the basic analysis of each variable. We then give an example of a short-term atmospheric event that shows the monitoring capacity of the network. This dataset, which is publicly available, is planned to be updated on a near-real time and should be valuable for climate change estimation, extreme weather events diagnosis, data assimilation, weather forecasting, etc. The dataset is available at https://doi.org/10.11888/Atmos.tpdc.272721 (Ding et al., 2022).

https://doi.org/10.5194/essd-2022-188
Preprint. Discussion started: 19 July 2022
© Author(s) 2022. CC BY 4.0 License.

1. Introduction

Antarctica, covered by a vast ice sheet, has the coldest climate on Earth's surface (Qin and Ren, 2001; Van den Broeke and Van Lipzig, 2003; Zhou et al., 2009). Great efforts have been made to study Antarctic climate change under global warming because of its role in the climate system and its capacity to greatly impact global sea level rise (IPCC, 2019; Huai et al., 2019). However, the reliability of Antarctic climate change estimation and weather forecasting is still under debate (Hines et al., 2019; Zhang et al., 2021). This is a consequence of the paucity of observations, especially at long term inland weather stations, which can be directly assimilated in to models and reanalysis data (Vignon et al., 2017; Wei et al., 2019).

The first attempt at automatic weather station (AWS) observations in Antarctica was in 1956/57, when station XG1 was deployed by the United States near McMurdo; but this station was short lived (Lazzara et al., 2012). Early attempts at AWS observations were also made off the coast of East Antarctica by the Australian National Antarctic Research Expedition (ANARE) at Chick Island (in 1961) and Lewis Island (in 1962). Both these stations were also short lived.

Development of automatic observational technology in polar regions was greatly advanced with initiation, in 1978, of the ARGOS data relay system on polar orbiting satellites. This, together with more robust and power-efficient electronics, saw successful Antarctic AWS deployments by the University of Wisconsin, USA, commencing in 1980. The Australian Antarctic Division also tested its design of AWS at near-coastal sites in 1980 and deployed its first successful station on the inland ice sheet, at 1830 m elevation, in January 1982 (Allison and Morrissey, 1983). Subsequently, more and more Antarctic AWSs were installed: ~30 by 1990, ~55 by 2000, ~60 by 2010 and ~160 by 2020 (Bromwich et al., 2020). Many of these were installed as part of a United States network on the Ross Ice Shelf, inland from the Adélie Land coast for a study of katabatic wind flow, and at other interior ice sheet sites (Lazzara et al., 2012). During the International Antarctic Glaciological Project traverses from Casey station, a number of ANARE AWSs were deployed on the ice sheet, along about 110°E to 3096 m elevation. Australian glaciological traverses between Mawson and Zhong Shan stations deployed 5 AWSs at 2500 m elevation around the interior of the Lambert Glacier Basin, between 1990 and 1994 (Allison 1998; Heil, 2006). Further west in eastern Dronning Maud Land, stations were built and deployed on the

https://doi.org/10.5194/essd-2022-188
Preprint. Discussion started: 19 July 2022
© Author(s) 2022. CC BY 4.0 License.

ice sheet by Japan at Dome Fuji (in December 1993) and Relay (in January 1993) (Enomoto et al.,1995). To extend knowledge of the near-surface climate and heat budget of Antarctica, Netherlands started to deploy AWSs in western Dronning Maud Land in January 1997 (Reijmer and Oerlemans, 2002).

Several of the AWSs mentioned failed after a relatively short time, and those in high accumulation near-coastal areas became buried by snow. But quite a few continued to provide high-quality data for many years. For example, the Australian AWS at GC41, inland of Casey at 2760 m elevation, provided good data for more than 21 years until eventually buried, although it was never visited for maintenance. The interior ice sheet with low accumulation, relatively low wind speeds, and no liquid water is actually a benign environment for electronic systems if properly designed for very low temperatures. The higher latitude sites also see more transits of polar-orbiting satellites carrying the ARGOS data relay system.

These AWS observations have made valuable contributions to Antarctic research. Firstly, the data have been used to evaluate weather and climate changes (Turner et al., 2005; 2007; Wei et al., 2019; Wang et al., 2022). For example, Schwerdtfeger (1984) gave a brief characterization of the inland Antarctica climate from AWS data. Allison et al (1993) analyzed the influence of ice sheet topography on surface meteorology using 10 AWSs from both the US-French network in Adélie Land and the Australian network inland of Casey. Secondly, AWS data, including radiation measurements, can be used to investigate ice/snow-atmosphere interaction processes in Antarctica. Van den Broeke et al. (2004a; 2004b; 2005; 2006) studied the daily and seasonal variation of the surface energy balance in detail in Dronning Maud Land. Ding et al. (2020; 2021a) improved the surface energy balance simulation scheme at Dome A and the inland Antarctic area with long term AWS measurements. Thirdly, AWS observations are also critical in evaluating the applicability of reanalysis data and numerical models in Antarctica. Nigro et al. (2011) estimated the performance of Antarctic Mesoscale Prediction System (AMPS) under varied synoptic conditions with AWS data for the Ross Ice Shelf. Xie et al (2014) assessed the accuracy of daily mean surface pressure from different meteorological reanalyzes against in situ observations from automatic weather stations in East Antarctica. Dong et al. (2020) evaluated the robustness of near-surface wind speed of multiple global atmospheric reanalysis in Antarctica based on many AWS and meteorological observations made at staffed stations. Recently, Wei et al. (2019) and Turner et al. (2020) used multiple meteorological records to give the

https://doi.org/10.5194/essd-2022-188
Preprint. Discussion started: 19 July 2022
© Author(s) 2022. CC BY 4.0 License.

spatial/temporal distribution of temperature extremes across Antarctica for the first time.

However, most staffed observational sites and AWSs in Antarctica are still mainly located in the coastal area, and data from the sparse inland sites is interrupted frequently (e.g., the anemometer was often frozen during austral winter at Eagle, Dome A) (Wendler et al., 1988; Van As et al., 2005; Zhou et al., 2009; Lazzara et al., 2012; Sun et al., 2018; Bromwich et al., 2020). More continuous and systematic AWS observation, are still required from Antarctica.

Commencing in 1996/1997 austral summer, the Chinese National Antarctic Research Expedition (CHINARE) started deploying AWSs between the coastal Zhongshan and inland Panda S (the PANDA transect).The first station deployed on this transect were manufactured by the Australian Antarctic Division, but after 2012, the Chinese Academy of Meteorological Sciences made great progress in AWS design, especially the ultra-low temperature power supply system (patent for invention, Ding et al., 2021b), and deployed 7 further AWSs along the PANDA transect.

Initial studies using these observations focused on the coastal area or a single site (e.g., van den Broeke et al., 2004a; 2004b; Chen et al., 2010) while later studies used data from more inland stations (Ma et al., 2010; Ding et al., 2021a). Only a few studies have used meteorological information from the whole transect (Zhou et al. 2009; Ma et al. 2010; Bian et al. 2016). That is because only 5 of the initial AWSs survived till 2012. These were Dome A, Eagle, and Panda N (Australian Antarctic Division), Zhongshan and Panda S (Chinese Academy of Meteorological Sciences). The more recent deployments now provide a consistent, high quality and real time meteorological observations from the PANDA AWS network. Some data from the PANDA AWS network have been compiled by WMO (e.g., Dome A ID: 89577, Eagle ID: 89578, Kunlun ID: 89572, Taishan ID: 89576) and some are available as monthly means from the Scientific Committee on Antarctic Research (SCAR) Reference Antarctic Data for Environmental Research (READER) (http://www.antarctica.ac.uk/met/READER/). But most of these data have not been published before. Here, in order to promote and make available the value of these AWSs data, we provide metadata of the dataset that will be updated on a near-real time in A Big Earth Data Platform for Three Poles (http://poles.tpdc.ac.cn/zh-hans/). We also provide an overview of the climate characteristics of the site.

https://doi.org/10.5194/essd-2022-188
Preprint. Discussion started: 19 July 2022
© Author(s) 2022. CC BY 4.0 License.

2 Observation region and data processing

2.1 Observation region and site descriptions

The PANDA transect is approximately along 77° E longitude, and stretches approximately 1460 km from the coast at Zhongshan to the dome region at Dome A, the summit of the East Antarctic Ice Sheet. This transect is highly representative of East Antarctica highly, for it covers Prydz Bay, Lambert Glacier/Amery Ice Shelf, high inland and dome regions. According to Zhang et al. (2008) and Ding et al. (2011), the PANDA transect can be divided into three typical topographies: a coastal region characterized by steep terrain (corresponding to Zhongshan to Panda 200), an inland region with strong katabatic wind (Panda 300 to Eagle), and a dome region (Panda 1100 to Panda S). The PANDA transect includes almost all the climate types in East Antarctica.

The PANDA AWS network had 11 AWSs in operation in 2022: Zhongshan, Panda 100, Panda 200 (LGB 69), Panda 300, Panda 400, Taishan, Eagle, Panda 1100, Dome A, Kunlun and Panda S. All of them are located on the western side of the Lambert Glacier Basin (Fig. 1), at different latitudes (69° S-83° S) and at different elevations (detailed information can be found in Table 1). The first site, Zhongshan was established in March 1989, when CHINARE first arrived in East Antarctica. It was initially a Staffed Weather Station but has now has replaced by an AWS. LGB 69 (192 km from the coast) was first deployed in January 2002 during the Lambert Glacier Basin traverse, but is buried every 3 years approximately. This area also has very rapid ice movement and high accumulation rate (Zhang et al., 2008; Ding et al., 2015), it is hard to rebuild it in exactly the same place. Thus, in December 2016, PANDA 200 was deployed 200 km from the coast and considered as a replacement AWS for LGB 69. In January 2005, Eagle and Dome A were installed during the CHINARE 21th which reached the summit of East Antarctic Ice Sheet, ~1248 km from the coast, the observed lowest air temperature was -80.36 °C (0300 UTC, 3 September 2007) at height of 4 m on Dome A. Then in January 2008, Panda S was deployed in cooperation with the University of Wisconsin as a contribution to the International Polar Year, but this AWS has been intermittent. The other AWSs were deployed during 2012 and 2019, and were manufactured by the Chinese Academy of Meteorological Sciences. The hourly data from the all AWSs are remotely collected and relayed in near real-time only by the ARGOS System and not saved internally.

https://doi.org/10.5194/essd-2022-188
Preprint. Discussion started: 19 July 2022
© Author(s) 2022. CC BY 4.0 License.

It should be noted that these AWSs are of several different designs for different scientific purposes. All include sensors for air temperature (T_a) and wind speed (*WS*), initially at 1, 2, 4 and/or 6 m height above surface (the surface height and station tilt are not part of the monitored variables, all sensors height in this paper is initial height from build stations), and wind direction (*WD*), relative humidity (*RH*) and air pressure (*P*). Panda 300, Taishan, Eagle and Dome A AWSs are also equipped with surface and firn temperature probes (detailed information can be found in Table 1). The Zhongshan is designed to WMO service regulation so the initial height of wind measurement is 10 m.

The Chinese Academy of Meteorological Sciences designed AWSs use a HMP155 resistance probe to measure air temperature and relative humidity; Panda S and which uses a Weed PRT 2-wire bridge and Vaisala HMP35A; and Eagle and Dome A use FS23D thermistors and HMP35D humidity probe (Xiao et al., 2008). The Eagle and Dome A have cup anemometers which stall during extreme austral winter cold (Zhou et al., 2009; Ma et al., 2010), but the other AWSs are equipped with XFY3-1 wind propeller anemometers and some of them are optimized to prevent “diamond dust “accumulation on the instruments. Details of the sensor and AWS schemes can be found in Table1.

All sensors are calibrated before fieldwork, but super cold weather below -60 ℃ may bring uncertainty. The height of the sensors above surface gradually decreases with snow accumulation, except for Zhongshan which is on rock. This has been ignored in the preliminary analysis presented here.

2.2 Data quality control

All data are checked initially to ensure integrity, consistent with the approach of Ma et al. (2010), Lazzara et al. (2012), and Wawrzyniak and Osuch (2020). Firstly, ARGOS reception may lead to duplicated records, time dislocation (Fig. 2) and these are removed. For those AWSs with measurements of air temperature and wind at multiple levels, a check of the vertical profiles is a particularly strong validation. If the vertical profiles are near logarithmic, then the absolute values are sure to be accurate. Secondly, different variables are compared to check their consistency. For instance, wind direction will be eliminated when wind speed is zero. In addition, the height of sensors might change with snow accumulating. The correction method to this error have been introduced in Ma et al. (2008) and Smeets et al. (2018). In addition, the logger box was buried in the snow at installation, which has the advantage of not interfering with the

https://doi.org/10.5194/essd-2022-188
Preprint. Discussion started: 19 July 2022
© Author(s) 2022. CC BY 4.0 License.

radiation measurement. Daily mean values are averaged from hourly data and then monthly and annual mean values are progressively calculated. Similarly to the methodology of Maturilli et al. (2013) and Zou et al. (2021), missing values are handled depending on their duration. If more than 21% data (5 hours) during one day, or 12% data (4 days) within one month, or 25% data (3 months) within one year are missing, the daily/monthly/annual data is considered a missing value.

The measurements at Zhongshan were made only four times a day (00:00, 06:00, 12:00 and 18:00, UTC) from 1 March 1989 to 31 January 2002., Hence we analyzed diurnal data only from 2002 to 2020 for consistency, but monthly/annual data from 1989 to 2020. The average of meteorological variables at other AWSs were calculated for different spans depending on their deployment dates, which are not the same (Table 1): Panda100, Panda 300, Panda 400 and Panda 1100 span from 2019 to 2021; Panda 200 spans from 2016 to 2021; Taishan spans from 2012 to 2021; Eagle and Dome A span from 2005 to 2020; Kunlun spans from 2017 to 2021; Panda S spans from 2008 to 2021. All variables are analyzed at a height of 4 m, except at Zhongshan, Panda 200 and Panda 400. The wind speed and direction at Zhongshan are at10 m height, and the air temperature and relative humidity at Panda 200 and Panda 1100 are at 6 m and 2 m heights, respectively.

Due to heavy hoar frost in the Antarctic inland, anemometer with a vertical axis was often frozen during austral winter at Eagle, Dome A and Panda S, which may lead to invalid measurements (Zhou et al., 2009). We used a different anemometer on the other AWSs and deleted the wintertime wind speed data for those three AWSs.

3 Results

3.1 Air temperature

Mean diurnal variation of air temperature is obviously an approximately sinusoidal curve at all AWSs (Fig. 3). The maximum air temperature occurs at 0900-1100 UTC (1400-1600, LST), and the minimum was at 2200-2300 UTC (0300-0400, LST). From the coast to dome area, the standard deviation of diurnal variations gradually increases (from 0.64 °C at Zhongshan to 1.42 °C at Panda S).

The monthly mean air temperatures all show a “coreless” winter with a single “valley” pattern; in other words, there is no distinctive minima during austral winter (Fig. 4). The variability (standard deviation of monthly air temperature) in austral winter is much larger than in austral summer, e.g., 2.46 °C vs 1.67 °C at Taishan. This indicates that

https://doi.org/10.5194/essd-2022-188
Preprint. Discussion started: 19 July 2022
© Author(s) 2022. CC BY 4.0 License.

the Antarctica Ice Sheet experiences more weather activities during austral winter. For example, sometime cyclones from the surrounding ocean may bring warm, moist air masses (Qin et al., 2017; Ding et al., 2020). In addition, the inland region exhibits more dynamic weather either than coast or the dome summit regions, coinciding with a larger standard deviation in monthly air temperature. This is 1.5 times (3.24 °C) that of the others two regions (2.19 °C, and 2.39 °C respectively).

With consideration of the length of the observation period, the trend in annual mean air temperatures is shown for only 4 AWSs in Fig. 5. These are Zhongshan (1989 to 2020), Taishan, (2013 to 2020) Eagle (2005 to 2020) and Dome A (2005 to 2020). They have annual means of -10.0 °C, -35.4 °C, -41.2 °C and -50.4 °C respectively, similar to the results of Ma et al. (2010). This difference can be attributed to differences in elevation/topography and latitude (Allison et al., 1993). The annual variations of air temperature at the four sites are multivariate. There has been a warming trend at Zhongshan of 0.10 °C/decade, and significant increase of air temperature at Taishan of 1.07 °C/decade. However, there has been no significant change at Eagle (-0.13 °C/decade) or Dome A (-0.07 °C/decade), unlike that at Vostok and South Pole which are experiencing warming (Clem et al., 2020).

3.2 Relative humidity

The variation of local atmospheric moisture is driven by a combination of large-scale advection and local evaporation/sublimation effects (Maturilli et al., 2013). Figure 6 shows a similar distribution to a previous study (Ma et al., 2010); the austral summer is more humid than the austral winter at all AWSs. However, coastal relative humidity fluctuates largely on the monthly scale but there is a little difference between austral summer and winter. At the inland and dome summit regions, the monthly relative humidity has a very clear seasonal cycle.

Figure 7 shows the annual averages and trends of relative humidity at Zhongshan, Taishan, Eagle and Dome A. Relative humidity varied considerably at all sites, with the driest records at Dome A. Interestingly, the relative humidity is well correlated with air temperature except at Zhongshan, partially because its weather is controlled by the adjacent ocean.

3.3 Air Pressure

Air pressure obviously decreases with elevation from coast to dome area, and the seasonal cycles also becomes clearer. Monthly mean air pressure shows a semi-annual oscillation with equinoctial minima near the coastal and inland areas along the PANDA AWS network, but is much less distinct at dome area, this semi-annual oscillation could be submerged under larger annual oscillation (Fig. 8) (Radok et al., 1996). Coastal areas like Zhongshan, Panda 100 and Panda 200 have little air pressure difference between austral summer and winter, but there are obvious differences inland area, with a stable-strong low-pressure structure at the plateau surface in austral winter. However, there are more cyclone activities in inland area (Panda 300 to Eagle) (Ding et al., 2020), showed by the highest standard deviation of air pressure, (705±4 hPa), higher than coastal (858±3.10 hPa) and dome areas (585±2.74 hPa). The annual averages (Table 2) and trend of air pressure at the AWS shows no systematic variation, consistent with Zhou et al. (2009) and most of the other studies in East Antarctica.

3.4 Wind speed and direction

Diurnal variation in wind speed shows most clearly in the coastal katabatic region (Fig. 9). The maximum wind speed occurs around 0400-0800 UTC (0900-1300 LST) and minimum around 1400-1600 UTC (1900-2100 LST at near-coastal AWSs. Diurnal variation of wind speed gradually decreases from the coast to the dome region, from Panda 1100 to Panda S, which showed very weak fluctuation because the dome area is a sink center for atmosphere circulation and the origin of Antarctic surface wind flow (Parish and Bromwich, 1987; Van den Broeke and Van Lipzig, 2003; Aristidi et al., 2005; Das et al., 2013). This phenomenon is also reflected in the vertical temperature gradient difference. At all times of day, the surface atmosphere has a positive temperature gradient (the 4 m air temperature is higher than 2 m). Thus, the wind is stable and weak at Dome A. Similarly, Zhou et al. (2009) and Bian et al. (2016) also found that there was persistent and stable inversion layer due to strong surface cooling of Antarctic ice sheet.

There is evidence of seasonal variations of wind speed at most AWSs. The austral winter wind speed is higher than austral summer (Fig. 10). This is related to the intensity of surface cooling and topography of the ice sheet. Wind flow can be accelerated by cooling along slope (Van den Broeke et al. 2002). The fluctuation of wind speed was much greater in austral winter than in summer, e.g., the standard deviations at Panda 200 were 1.43 m s^{-1} and 0.99 m s^{-1} in austral winter and summer respectively. From the coast to dome area, the wind speed became weaker, which has also been discussed by

https://doi.org/10.5194/essd-2022-188
Preprint. Discussion started: 19 July 2022
© Author(s) 2022. CC BY 4.0 License.

Ma and Bian (2014) and can be attributed to the katabatic effect. Zhongshan is an exception, its wind speed is weaker than at the other coastal AWSs. This AWS was deployed on rock at the edge of Antarctica whose katabatic effect was weakened. This pattern is also coincidence with aerodynamic roughness length, momentum transfer coefficient and friction velocity (Van den Broeke et al., 2002; Zhou et al., 2009, Ma et al., 2010).

In the long-term, the wind speed showed a weakening trend over the whole transect (Fig. 11). The trend at Zhongshan was -0.41 m s^{-1}/decade ($p < 0.01$) from 1989 to 2020 and there was also a decrease at Taishan (-0.08 m s^{-1}/decade) from 2013 to 2020. This phenomenon deserves future investigation.

As has been previously noted, the vertical axis anemometers of Dome A and Eagle are often frozen during austral winter, and the data quality of wind during austral fall is poor. Therefore, we analyzed wind direction in only the half year (September-February) at these two sites. Figure 1 showed the wind rose distribution of all AWSs. The wind directions at coastal and inland areas (from Zhongshan to Taishan) were relatively stable: during austral summer, constant easterlies determine the ice sheet surface wind, which is thus mainly from NE to SE. In austral winter, katabatic forcing from strong surface cooling, large-scale pressure gradient and Coriolis force, dominates, it also showed from NE to SE (Van den Broeke et al., 2002; Van den Broeke and Van Lipzig, 2003). At the dome summit region, the wind direction has a broad distribution with weak wind speed south, southeast and west. Especially at the Dome A, no prevailing wind has showed from ~18 years observation.

4. Capability of monitoring short-term atmospheric events

Compared to other meteorological observations, one advantage of the PANDA AWS network is that it covers all terrain and climatic sectors of East Antarctica. The local weather condition can be reflected from the meteorological surface measurements. Figure 12 shows the course of air pressure, air temperature, relative humidity and wind speed on 30th July-3rd August 2020, which indicates the occured of prominent blocking event. To assess the capability to monitor weather conditions, this physical atmospheric process was analyzed by PANDA AWSs network dataset.

On 1st August 2020, the blocking stretched southward to around 100°E, forming a high-pressure ridge in the interior of ice sheet (not shown). The deep low-pressure system was blocked from moving eastward and thus stagnated near Prydz Bay. This

https://doi.org/10.5194/essd-2022-188
Preprint. Discussion started: 19 July 2022
© Author(s) 2022. CC BY 4.0 License.

situation facilitated the meridional advection of warm, moist air masses. It can be seen in Fig. 12, that the air temperature, relative humidity, air pressure and wind speed from Zhongshan to Dome A changed with the development of the event. The uppermost site to detect the blocking is Dome A with 4093 m a.s.l. and the average speed of the blocking event across transect was about 40 km/h. Before 1st August, there was a drastic drop in air pressure at AWSs from Zhongshan to Taishan, reaching the lowest value at noon, but the air pressure from Eagle to Dome A showed no such changes. Meanwhile, the air temperature, relative humidity and wind speed show the opposite change at all AWSs, rising sharply and reaching the highest value at noon, average rose nearly 26%, 19% and 173% (compared with the time from 30th July to before the blocking event), respectively, indicative of maritime air intrusions to PANDA transect. On 3 August, the deep low-pressure system was slightly weaker (not shown). The southern section of the Indian Ocean subtropical high became flat in the geopotential height field, and blocking event move eastward and eventually dissipate along the coast or over the ocean surface. This event was similar to a recent abrupt warming event in Dome C (Ding et al., 2022a). Therefore, the PANDA AWS network provides high spatial-temporal observations and can play an important role in short-term weather forecast on the Antarctic Ice Sheet.

5. Data availability

This dataset is publicly available and it is planned that it will be updated on a near-real time. The data from the other AWSs will be publicly available on the A Big Earth Data Platform for Three Poles, the links are as follows: Zhongshan, Panda 100, Panda 200, Panda 300, Panda 400, Taishan, Panda 1100 and Kunlun The data can be downloaded from https://doi.org/10.11888/Atmos.tpdc.272721 (Ding et al., 2022b).

6. Conclusion

In this paper, we have introduced the PANDA AWS network which can monitor the meteorology from Zhongshan to beyond Panda S with high spatial and temporal resolution. The data collected during the past decades are reliable after calibration and homogenization, and have been used widely in meteorological and climate change research in Antarctica (e.g., Xie et al., 2016, Ding et al. 2021a). The data can also be used to derive surface energy balance, assimilated into reanalyzes, and used to evaluate climate models and to validate satellite data.

In a preliminary analysis, the diurnal, monthly, annual average and the long-term

https://doi.org/10.5194/essd-2022-188
Preprint. Discussion started: 19 July 2022
© Author(s) 2022. CC BY 4.0 License.

changes of air temperature, relative humidity, air pressure, wind speed and direction have been presented. They show significant differences between coastal, inland and dome summit regions. An example has also been given of a short-term atmospheric process to show this dataset's capability for weather monitoring and investigating.

Author contributions.

MD, IA and XZ designed the experiments and wrote the manuscript; MD carried out the experiments; XZ and DY analyzed the experimental results. MD, XZ, PH and DY revised the manuscript; CL, QS and WZ provides the information of AWS; DY, LB and CX discussed the results.

Competing interests.

The authors declare that they have no conflict of interest.

Acknowledgements.

The observations and AWS deployments were carried out during the Chinese National Antarctic Research Expedition from Zhongshan to Kunlun. We are grateful to David Mikolajczyk from Antarctic Meteorological Research and Data Center at the University of Wisconsin for providing meteorological data and AWS information for Panda S.

Financial support.

This research has been supported by the National Science Foundation of China (42122047), the National Key Research and Development Program of China (2021YFC2802504) and Basic fund of CAMS (2021Z006).

https://doi.org/10.5194/essd-2022-188
Preprint. Discussion started: 19 July 2022
© Author(s) 2022. CC BY 4.0 License.

Open Access Earth System Science Data Discussions

Reference

Aristidi, E., Agabi, K., Azouit, M., Fossat, E., Vernin, J., Travouillon, T., Lawrence, J. S., Meyer, C., Storey, J. W. V., Halter, B., Roth, W. L., and Walden, V.: An analysis of temperatures and wind speeds above Dome C, Antarctica. Astronomy & Astrophysics, 430(2), 739-746, https://doi.org/10.1051/0004-6361:20041876, 2005.

Allison, I. and Morrissy, J.V.: Automatic weather stations in Antarctica. Australian Meteorological Magazine, 31(2),71-76, 1983.

Allison, I., Wendler, G., and Radok, U.: Climatology of the East Antarctic ice sheet (100°E to 140°E) derived from automatic weather stations, Journal of Geophysical Research: Atmospheres, 98(D5), 8815-8823, https://doi.org/10.1029/93JD00104, 1993.

Bian, L., Allison, I., Xiao, C., Ma, Y., Fu, L., and Ding, M.: Climate and meteorological processes of the East Antarctic ice sheet between Zhongshan and Dome-A, Advances in Polar Science, 27(2), 90-101, https://doi.org/10.13679/j.advps.2016.2.00090, 2016.

Bromwich, D. H., Werner, K., Casati, B., Powers, J. G., Gorodetskaya, I. V., Massonnet, F., Vitale, V., Heinrich, V. J., Liggett, D., Arndt, S., Barja, B., Bazile, E., Carpentier, S., Carrasco, J. F., Choi, T., Choi, Y., Colwell, S. R., Cordero, R. R., Gervasi, M., Haiden, T., Hirasawa, Na., Inoue, J., Jung, T., Kalesse, H., Kim, S.J., Lazzara, M. A., Manning, K. W., Norris, K., Park, S. J., Reid P.,, Rigor, I., Rowe, P. M., Schmithüsen, H., Seifert, P., Sun, Q., Uttal, T., Zannoni, M., and Zou, X.: The Year of Polar Prediction in the Southern Hemisphere (YOPP-SH), Bulletin of the American Meteorological Society, 101(10), E1653-E1676, https://doi.org/10.1175/BAMS-D-19-0255.1, 2020.

Chen, B., Zhang, R., Xiao, C., Bian, L., and Zhang, T.: Analyses on the air and snow temperatures near ground with observations of an AWS at Dome A, the summit of Antarctic Plateau, Chinese Science Bulletin, 55(11), 1048-1054, https://doi.org/10.1007/s11434-010-0099-1, 2010.

Clem, K.R., Fogt, R.L., Turner, J., Lintner B. R., Marshall G. J., Miller, J. R., and Renwick, J. A.: Record warming at the South Pole during the past three decades, Nature Climate Chang. 10, 762–770, https://doi.org/10.1038/s41558-020-0815-z, 2020.

Das, I., Bell, R. E., Scambos, T. A., Wolovick, M., Creyts, T. T., Studinger, M., Frearson,

https://doi.org/10.5194/essd-2022-188
Preprint. Discussion started: 19 July 2022
© Author(s) 2022. CC BY 4.0 License.

N., Nicolas, J. P., Lenaerts, J. T. M., and Van Den Broeke, M. R.: Influence of persistent wind scour on the surface mass balance of Antarctica. Nature Geoscience, 6(5), 367-371 https://doi.org/10.1038/ngeo1766, 2013.

Ding, M., Xiao, C., Li, Y., Ren, J., Hou, S., Jin, B., and Sun, B.: Spatial variability of surface mass balance along a traverse route from Zhongshan station to Dome A, Antarctica, Journal of Glaciology, 57(204), 658-666, https://doi.org/10.3189/002214311797409820, 2011.

Ding, M., Xiao, C., Li, C., Qin, D., Jin, B., Shi, G., Xie, A., and Cui, X.: Surface mass balance and its climate significance from the coast to Dome A, East Antarctica, Science China Earth Sciences, 58(10), 1787-1797, https://doi.org/10.1007/s11430-015-5083-9, 2015.

Ding, M., Yang, D., Van den Broeke, M. R., Allison, I., Xiao, C., Qin, D., and Huai, B.: The surface energy balance at Panda 1 station, Princess Elizabeth Land: A typical katabatic wind region in East Antarctica, Journal of Geophysical Research: Atmospheres, 125(3), e2019JD030378, https://doi.org/10.1029/2019JD030378, 2020.

Ding, M., Zhang, T., Yang, D., Allison, I., Dou, T., and Xiao, C.: Brief communication: Evaluation of multiple density-dependent empirical snow conductivity relationships in East Antarctica, Cryosphere, 15, 4201-4206, https://doi.org/10.5194/tc-15-4201-2021, 2021a.

Ding, M., Du, F., Zhang, W., Wen, H., and Lu, C.: Battery system adapted to polar ultra-low temperature environment and its temperature control method, Beijing: CN113659246A, 2021b.

Ding, M., Xiao, C., and Qin, D.: Explosive warming event in Antarctica on 18 March 2022 and its possible causes. Advances in Climate Change Research, https://doi.org/10.12006/j.issn.1673-1719.2022.068, 2022a.

Ding, M., Zou, X., Sun, Q., Yang, D., Zhang, W., Bian, L., Lu, C., Allison, I., Heil, P., and Xiao, C.: The PANDA automatic weather station network between the coast and Dome A, East Antarcitca (1989-2021). A Big Earth Data Platform for Three Poles, https://doi.org/10.11888/Atmos.tpdc.272721, 2022b.

Dong, X., Wang, Y., Hou, S., Ding, M., Yin, B., and Zhang, Y.: Robustness of the recent global atmospheric reanalyses for Antarctic near-surface wind speed climatology, Journal of Climate, 33(10), 4027-4043, https://doi.org/10.1175/JCLI-D-19-0648.1, 2020.

https://doi.org/10.5194/essd-2022-188
Preprint. Discussion started: 19 July 2022
© Author(s) 2022. CC BY 4.0 License.

Enomoto, H., Warashina, H., Motoyama, H., Takahashi, S., and Koike, J.: Data-logging automatic weather station along the traverse route from Syowa Station to Dome Fuji, Proc. of the NIPR Symp. on Polar Meteorol. and Glaciol., 9, 66-75, https://doi.org/10.15094/00003880, 1995.

Heil, P.: Atmospheric conditions and fast ice at Davis, East Antarctica: A case study. Journal of Geophysical Research: Oceans, 111(C5), https://doi.org/10.1029/2005JC002904, 2006.

Hines, K. M., Bromwich, D. H., Wang, S. H., Silber, I., Verlinde, J., and Lubin, D.: Microphysics of summer clouds in central West Antarctica simulated by the Polar Weather Research and Forecasting model (WRF) and the Antarctic Mesoscale Prediction System (AMPS), Atmospheric Chemistry and Physics, 19(19), 12431-12454, https://doi.org/10.5194/acp-19-12431-2019, 2019.

Huai, B., Wang, Y., Ding, M., Zhang, J., and Dong, X.: An assessment of recent global atmospheric reanalyses for Antarctic near surface air temperature, Atmospheric Research, 226, 181-191, https://doi.org/10.1016/j.atmosres.2019.04.029, 2019.

Intergovernmental Panel on Climate Change.: IPCC special report on the ocean and cryosphere in a changing climate, https://archive.ipcc.ch/srocc/, 2019.

Lazzara, M. A., Weidner, G. A., Keller, L. M., Thom, J. E., and Cassano, J. J.: Antarctic automatic weather station program: 30 years of polar observation, Bulletin of the American Meteorological Society, 93(10), 1519-1537, https://doi.org/10.1175/BAMS-D-11-00015.1, 2012.

Ma, Y., Bian, L., Xiao, C., Allison, I.: Correction of snow accumulation impacted on air temperature from automatic weather station on the Antarctic Ice Sheet. Advance in Polar Science, 20(04): 299-309, http://ir.casnw.net/handle/362004/7877, 2008.

Ma, Y., Bian, L., Xiao, C., Allison, I., and Zhou, X.: Near surface climate of the traverse route from Zhongshan Station to Dome A, East Antarctica, Antarctic Science, 22(4), 443-459, https://doi.org/10.1017/S0954102010000209, 2010.

Ma, Y., and Bian, L.: A Surface Climatological Validation of ERA-interim Reanalysis and NCEP FNL Analysis over East Antarctic, Chinese Journal of Polar Research, 26(4), 469-480, https://doi.org/10.13679/j.jdyj.2014.4.469, 2014.

Maturilli, M., Herber, A., and König-Langlo, G.: Climatology and time series of surface meteorology in Ny-Ålesund, Svalbard, Earth System Science Data, 5(1), 155-163, https://doi.org/10.5194/essd-5-155-2013, 2013.

Nigro, M. A., Cassano, J. J., and Seefeldt, M. W.: A weather-pattern-based approach to evaluate the Antarctic Mesoscale Prediction System (AMPS) forecasts: Comparison to automatic weather station observations, Weather and Forecasting, 26(2), 184-198, https://doi.org/10.1175/2010WAF2222444.1, 2011.

Parish, T., and Bromwich, D.: The surface wind-field over the Antarctic ice sheets, Nature 328, 51-54, https://doi.org/10.1038/328051a0, 1987.

Qin, D., and Ren, J.: The Antarctic Glaciology, Science Press, 2001.

Qin, T., Wei, L., and Ling, C.: The statistic and variance of cyclones enter in scientific investigation station of China in Antarctic, Acta. Oceanologica Sinica, 39(5), 44-60, https://doi.org/10.3969/j.issn.0253-4193.2017.05.005, 2017.

Radok, U., Allison, I. and Wendler, G.: Atmospheric surface pressure over the interior of Antarctica. Antarctic Science, 8(2), 209-217, 1996.

Reijmer, C. H., and Oerlemans, J.: Temporal and spatial variability of the surface energy balance in Dronning Maud Land, East Antarctica, Journal of Geophysical Research: Atmospheres, 107(D24), ACL-9, https://doi.org/10.1029/2000JD000110, 2002.

Schwerdtfeger, W.: Weather and climate of the Antarctic, New York: Elsevier Science, 1984.

Smeets, P. C., Kuipers Munneke, P., Van As, D., van den Broeke, M. R., Boot, W., Oerlemans, H., Snellen, H., Reijmer, C.H., and van de Wal, R. S.: The K-transect in west Greenland: Automatic weather station data (1993-2016), Arctic, Antarctic, and Alpine Research, 50(1), S100002, https://doi.org/10.1080/15230430.2017.1420954, 2018.

Sun, Q. Z., Zhang, L., Meng, S., Shen, H., Ding, Z. M., and Zhang, Z. H.: Meteorological observations and weather forecasting services of the CHINARE, Adv Polar Sci, 28 (4), 291-299, https://doi.org/10.13679/j.advps.2018.4.00291, 2018.

Turner, J., Colwell, S. R., Marshall, G. J., Lachlan-Cope, T. A., Carleton, A. M., Jones, P. D., Lagun V., Reid P. A., and Iagovkina, S.: Antarctic climate change during the last 50 years, International Journal of Climatology, 25(3), 279-294, https://doi.org/10.1002/joc.1130, 2005.

Turner, J., Overland, J. E., and Walsh, J. E.: An Arctic and Antarctic perspective on recent climate change, International Journal of Climatology: A Journal of the Royal Meteorological Society, 27(3), 277-293, https://doi.org/10.1002/joc.1406, 2007.

Turner, J., Marshall, G. J., Clem, K., Colwell, S., Phillips, T., and Lu, H.: Antarctic temperature variability and change from station data. International Journal of Climatology, 40(6), 2986-3007, https://doi.org/10.1002/joc.6378, 2020.

https://doi.org/10.5194/essd-2022-188
Preprint. Discussion started: 19 July 2022
© Author(s) 2022. CC BY 4.0 License.

Van As, D., Van den Broeke, M. R., and Van De Wal, R.: Daily cycle of the surface layer and energy balance on the high Antarctic Plateau, Antarctic Science, 17(1), 121-133, https://doi.org/10.1017/S095410200500252X, 2005.

Van den Broeke, M. R., Van Lipzig, N. P. M., and Van Meijgaard, E.: Momentum budget of the East Antarctic atmospheric boundary layer: Results of a regional climate model, Journal of the Atmospheric Sciences, 59(21), 3117-3129, https://doi.org/10.1175/1520-0469(2002)059<3117:MBOTEA>2.0.CO;2, 2002.

Van den Broeke, M. R., and Van Lipzig, N. P. M.: Factors controlling the near-surface wind field in Antarctica, Monthly Weather Review, 131(4), 733-743, https://doi.org/10.1175/1520-0493(2003)131<0733:FCTNSW>2.0.CO;2, 2003.

Van den Broeke, M. R., Reijmer, C. H., and Van De Wal, R.: Surface radiation balance in Antarctica as measured with automatic weather stations, Journal of Geophysical Research: Atmospheres, 109(D9), https://doi.org/10.1029/2003JD004394, 2004a.

Van den Broeke, M. R., Reijmer, C. H., and Van De Wal, R. S.: A study of the surface mass balance in Dronning Maud Land, Antarctica, using automatic weather stations, Journal of Glaciology, 50(171), 565-582, https://doi.org/10.3189/172756504781829756, 2004b.

Van den Broeke, M. R., Reijmer, C. H., Van As, D., Van de Wal, R., and Oerlemans, J.: Seasonal cycles of Antarctic surface energy balance from automatic weather stations, Annals of Glaciology, 41, 131-139, https://doi.org/10.3189/172756405781813168, 2005.

Van Den Broeke, M. R., Reijmer, C. H., Van As, D., and Boot, W.: Daily cycle of the surface energy balance in Antarctica and the influence of clouds, International Journal of Climatology: A Journal of the Royal Meteorological Society, 26(12), 1587-1605, https://doi.org/10.1002/joc.1323, 2006.

Vignon, E., Genthon, C., Barral, H., Amory, C., Picard, G., Gallée, H., Casasanta, G., and Argentini, S.: Momentum-and heat-flux parametrization at Dome C, Antarctica: A sensitivity study, Boundary-Layer Meteorology, 162(2), 341-367, https://doi.org/10.1007/s10546-016-0192-3, 2017.

Wang, S., Ding, M., Liu, G., Wei, T., Zhang, W., Chen, W., Dou, T., and Xiao, C.: On the Drivers of Temperature Extremes on the Antarctic Peninsula During Austral Summer, Climate Dynamics, https://doi.org/10.1007/s00382-022-06209-0, 2022.

Wawrzyniak, T., and Osuch, M.: A 40-year High Arctic climatological dataset of the Polish Polar Station Hornsund (SW Spitsbergen, Svalbard), Earth System Science

https://doi.org/10.5194/essd-2022-188
Preprint. Discussion started: 19 July 2022
© Author(s) 2022. CC BY 4.0 License.

Data, 12(2), 805-815, https://doi.org/10.5194/essd-12-805-2020, 2020.

Wei, T., Yan, Q., and Ding, M.: Distribution and temporal trends of temperature extremes over Antarctica, Environmental Research Letters, 14(8), 084040, https://doi.org/10.1088/1748-9326/ab33c1, 2019.

Wendler, G., Ishikawa, N., and Kodama, Y.: The heat balance of the Icy slope of Adelie Land, Eastern Antarctica, Journal of Applied Meteorology, 27(1), 52-65, https://doi.org/10.1175/1520-0450(1988)027<0052:THBOTI>2.0.CO;2, 1988.

Xiao, C., Li, Y., Allison, I., Hou, S., Dreyfus, G., Barnola, J. M., Ren, J., Bian, L., Zhang, S., and Kameda, T.: Surface characteristics at Dome A, Antarctica: first measurements and a guide to future ice-coring sites, Annals of Glaciology, 48, 82-87, https://doi.org/10.3189/172756408784700653, 2008.

Xie, A., Allison, I., Xiao, C., Wang, S., Ren, J., and Qin, D.: Assessment of surface pressure between Zhongshan and Dome A in East Antarctica from different meteorological reanalyses. Arctic, Antarctic, and Alpine Research, 46(3), 669-681, https://doi.org/10.1657/1938-4246-46.3.669, 2014.

Xie, A., Wang, S., Xiao, C., Kang, S., Gong, J., Ding, M., Li, C., Dou, T., Ren, J., and Qin, D.: Can temperature extremes in East Antarctica be replicated from ERA Interim reanalysis? Arctic, Antarctic, and Alpine Research, 48(4), 603-621, https://doi.org/10.1657/AAAR0015-048, 2016.

Zhang, S., E, D., Wang, Z., Li, Y., Jin, B., and Zhou, C.: Ice velocity from static GPS observations along the transect from Zhongshan station to Dome A, East Antarctica, Annals of Glaciology, 48, 113-118, https://doi.org/10.3189/172756408784700716, 2008.

Zhang, Y., Wang, Y., and Hou, S.: Reliability of Antarctic air temperature changes from Polar WRF: A comparison with observations and MAR outputs, Atmospheric Research, 105967, https://doi.org/10.1016/j.atmosres.2021.105967, 2021.

Zhou, M., Zhang, Z., Zhong, S., Lenschow, D., Hsu, H. M., Sun, B., Gao, Z., Li, S., Bian, X., and Yu, L.: Observations of near-surface wind and temperature structures and their variations with topography and latitude in East Antarctica, Journal of Geophysical Research: Atmospheres, 114(D17), https://doi.org/10.1029/2008JD011611, 2009.

Zou, X., Ding, M., Sun, W., Yang, D., Liu, W., Huai, B., Jin, S., and Xiao, C.: The surface energy balance of Austre Lovénbreen, Svalbard, during the ablation period in 2014, Polar Research, 40, https://doi.org/10.33265/polar.v40.5318, 2021.

https://doi.org/10.5194/essd-2022-188
Preprint. Discussion started: 19 July 2022
© Author(s) 2022. CC BY 4.0 License.

Figures and Table:

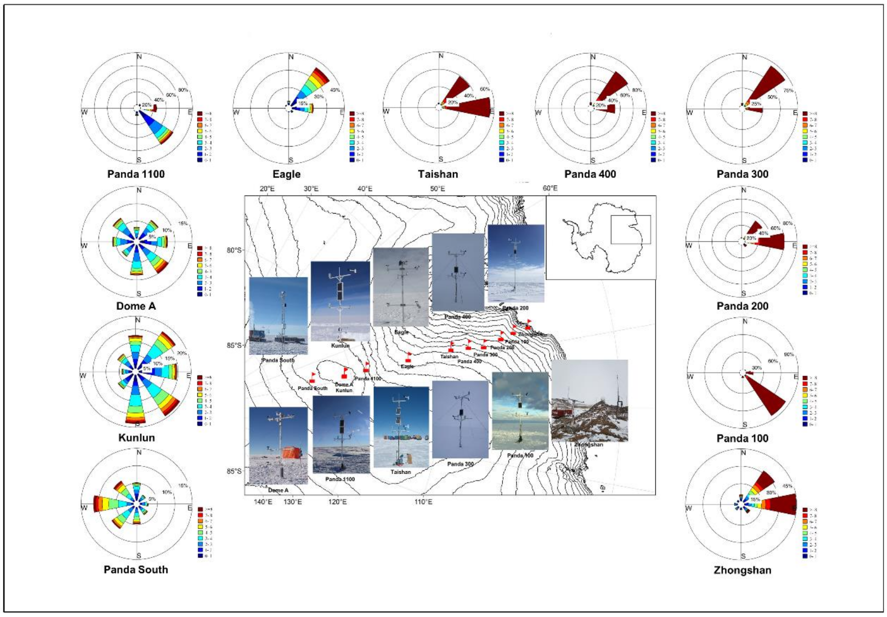

Figure 1. The location and Wind roses of AWSs in the PANDA network. The red flags are AWSs; the black solid lines are 200m interval contours. The wind directions are divided into 22.5° sectors. Zhongshan is calculated during 1989-2020; Panda 100, Panda 300 and Panda 400 are calculated during 2019-2021; Panda 200 is calculated during 2016-2021; Taishan is calculated during 2012-2021; Eagle and Dome A are calculated during 2005-2020; Kunlun is calculated during 2017-2021; and Panda S is calculated during 2008-2021. Note however that, because some winter data were unreliable, Eagle averages exclude Mar-Aug; Dome A averages exclude March-October; and Panda S averages exclude May-September.

https://doi.org/10.5194/essd-2022-188
Preprint. Discussion started: 19 July 2022
© Author(s) 2022. CC BY 4.0 License.

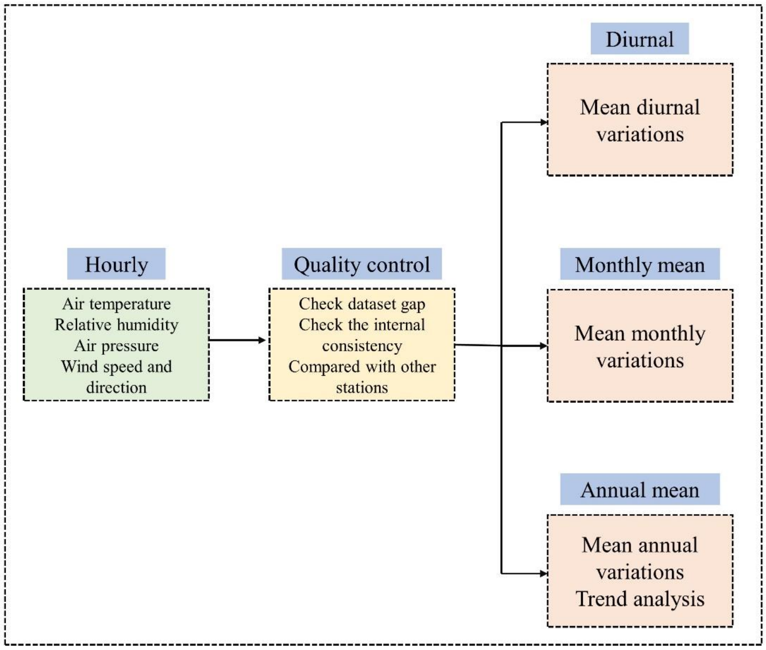

Figure 2. Schematic diagram of data processing workflow used to compile the AWS meteorology dataset for the network

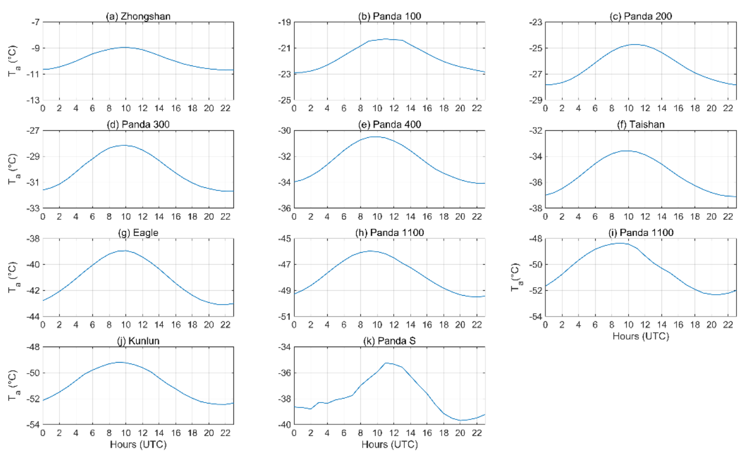

Figure 3. Average diurnal variation of air temperature at AWSs in the PANDA network. The calculation years for these sites are the same as in Fig. 1, excepting that Zhongshan is calculated during 2002-2020.

https://doi.org/10.5194/essd-2022-188
Preprint. Discussion started: 19 July 2022
© Author(s) 2022. CC BY 4.0 License.

Open Access Earth System Science Data Discussions

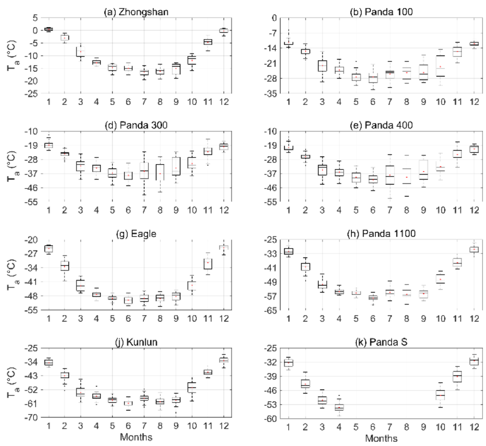

Figure 4. Variation of monthly mean air temperature at AWSs in the PANDA network. The calculation periods for these sites are the same as in Fig. 3, For each monthly box, the central line indicates the median, the red dot represents the mean, and the bottom and top edges of the box indicate the 25th and 75th percentiles, respectively.

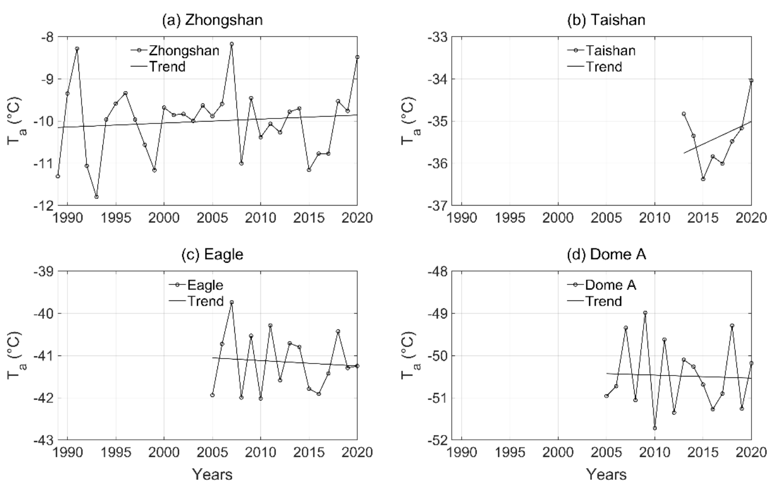

Figure 5. Variation of annual mean air temperature at Zhongshan, Taishan, Eagle and Dome A. Zhongshan is calculated during 1989-2020; Taishan is calculated during 2013-2020; Eagle and Dome A are calculated during 2005-2020.

https://doi.org/10.5194/essd-2022-188
Preprint. Discussion started: 19 July 2022
© Author(s) 2022. CC BY 4.0 License.

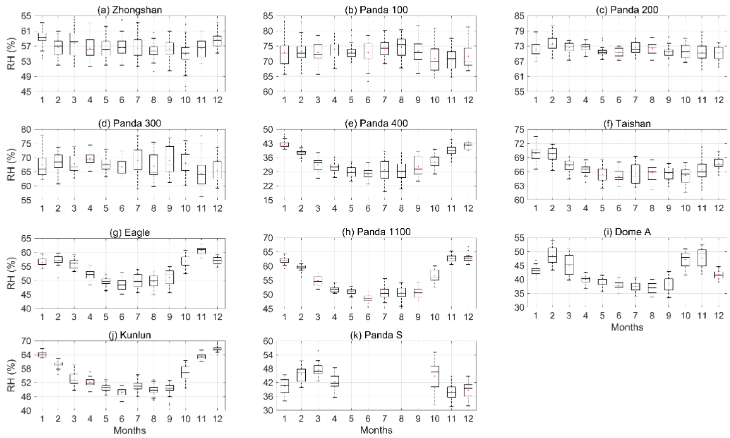

Figure 6. Monthly variation of relative humidity at AWSs in the PANDA network. The calculation periods of these sites are the same as in Fig. 3.

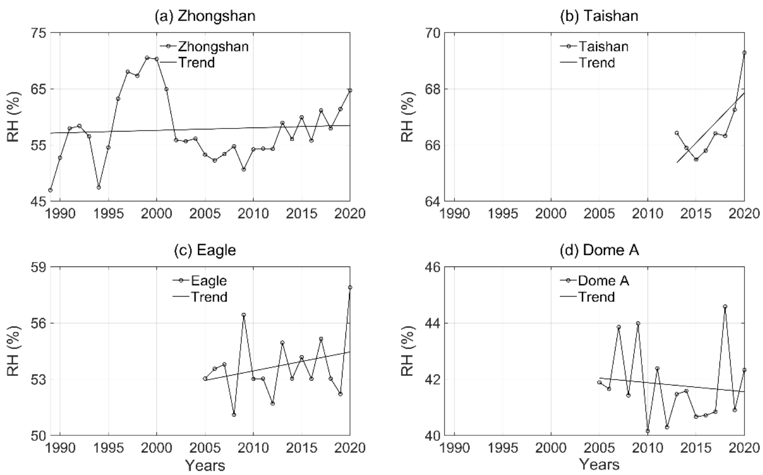

Figure 7. Annual variation of relatively humidity at Zhongshan, Taishan, Eagle and Dome A.

https://doi.org/10.5194/essd-2022-188
Preprint. Discussion started: 19 July 2022
© Author(s) 2022. CC BY 4.0 License.

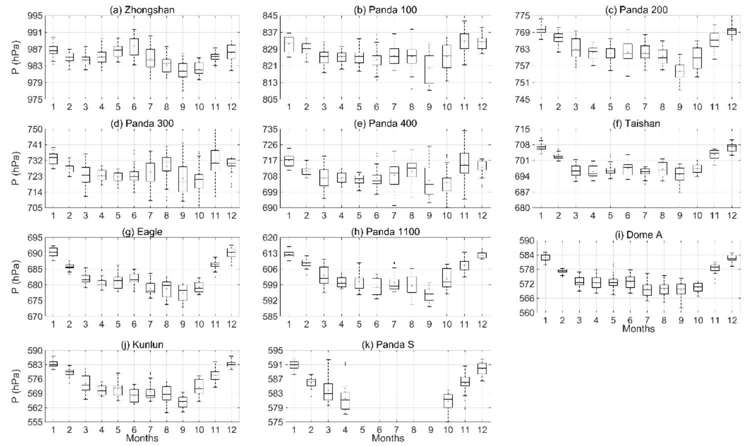

Figure 8. Monthly variation of air pressure at AWSs in the PANDA network. The calculation periods at these sites are the same as in Fig. 3.

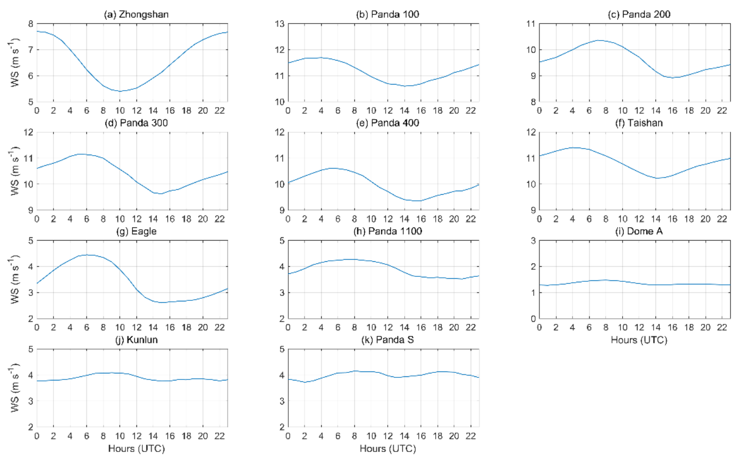

Figure 9. Diurnal variation of wind speed of PANDA AWSs network. The calculation periods of these site are the same with Fig. 1, Zhongshan is calculated during 2002-2020.

© Author(s) 2022. CC BY 4.0 License.

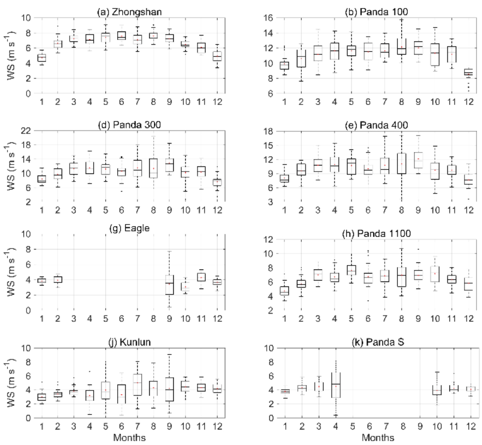

Figure 10. Monthly variation of wind speed of PANDA AWSs network. The calculation periods of these sites are the same with Fig. 1.

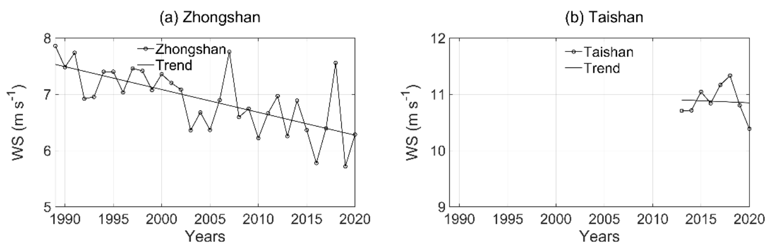

Figure 11. Annual variation of wind speed at Zhongshan and Taishan. The calculation periods of these site are the same with Fig. 5.

https://doi.org/10.5194/essd-2022-188
Preprint. Discussion started: 19 July 2022
© Author(s) 2022. CC BY 4.0 License.

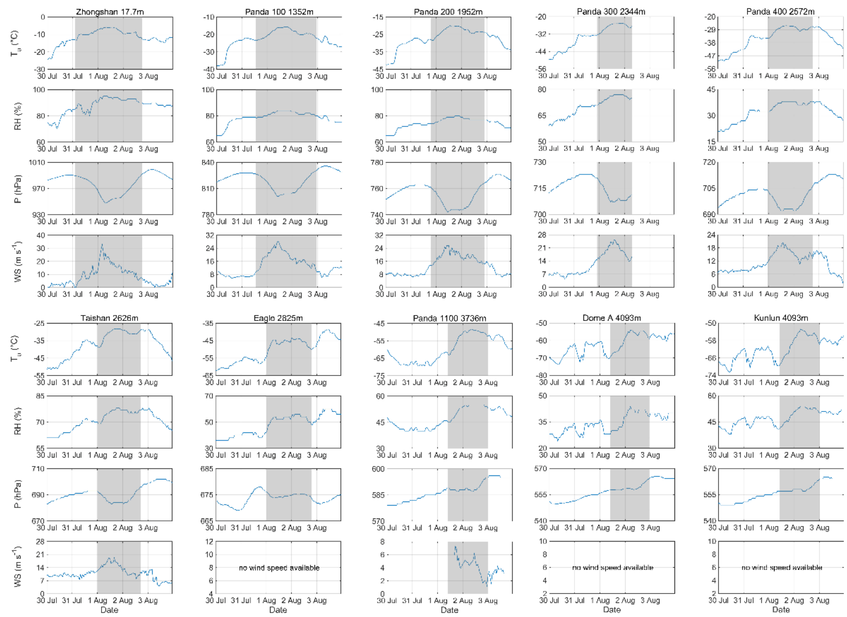

Figure 12. Changes in air temperature, relative humidity, air pressure and wind speed at AWS of the PANDA network (except Panda S) from 00:00 30th July to 23:00 3rd August 2020 (UTC); gray zone: block event.

https://doi.org/10.5194/essd-2022-188
Preprint. Discussion started: 19 July 2022
© Author(s) 2022. CC BY 4.0 License.

Open Access Earth System Science Data Discussions

Table 1. Locations, operational periods, observed variables and heights, and instrumentation and accuracies of AWSs in the PANDA network

Stations	Location	Altitude	Period(Y/M)	Variable	Sensor	Accuracy	Height
Zhongshan	69.37°S 76.38°E	17.7 m a.s.l.	1989/03-2020/12	Ta/RH	HMP155	(0.2260-0028*Ta) °C/1%	2m
				P	CS106	1.5hPa	2m
				WS/WD	XFY3-1	1m s^{-1}/5°	10m
Panda 100	70.22°S 76.65°E	1352 m a.s.l.	2019/02-2021/07	Ta/RH	HMP155	(0.2260-0028*Ta) °C/1%	2/4m
				P	PTB110	0.3hPa	2m
				WS/WD	XFY3-1	1m s^{-1}/5°	2/4m
				SDR/SUR	Li200X	5% Max/3% Typical	2m
Panda 200	70.97°S 77.19°E	1952 m a.s.l.	2016/12-2021/07	Ta/RH	HMP155	(0.2260-0028*Ta) °C/1%	4/6m
				P	PTB210	0.5hPa	4m
				WS/WD	XFY3-1	1m s^{-1}/5°	4/6m
				SDR/SUR	Li200X	5% Max/3% Typical	4m
Panda 300	72.00°S 77.95°E	2344 m a.s.l.	2019/12-2021/07	Ta/RH	HMP155	(0.2260-0028*Ta) °C/1%	2/4m
				P	PTB210	0.5hPa	2/4m
				WS/WD	XFY3-1	1m s^{-1}/5°	2/4m
				SDR/SUR	Li200X	5% Max/3% Typical	2m
Panda 400	72.86°S 77.38°E	2572 m a.s.l.	2019/12-2021/07	Ta/RH	HMP155	(0.2260-0028*Ta) °C/1%	1/2/4m
				P	PTB210	0.5hPa	2m
				WS/WD	XFY3-1	1m s^{-1}/5°	1/2/4m
				SDR/SUR/LDR/LUR	Li200X	5% Max/3% Typical	2m
Taishan	73.86°S 76.98°E	2626 m a.s.l.	2012/12-2021/07	Ta/RH	HMP155	(0.2260-0028*Ta) °C/1%	2/4m
				P	PTB110	0.3hPa	2m
				WS/WD	XFY3-1	1m s^{-1}/5°	2/4m
				SDR/SUR	CNR4	10%	2m
Eagle	76.42°S 77.02°E	2825 m a.s.l.	2005/01-2020/12	Ta	FS23D	0.05°C	1/2/4m
				RH	HMP35D	2%	2m
				P	6015A	0.5hPa	2m

https://doi.org/10.5194/essd-2022-188
Preprint. Discussion started: 19 July 2022
© Author(s) 2022. CC BY 4.0 License.

				WS/WD	12170C/3590B	0.5m s^{-1}/6°	1/2/4m
Panda 1100	79.01°S 76.99°E	3736 m a.s.l.	2019/01- 2021/07	Ta/RH	HMP155	(0.2260- 0028*Ta) °C/1%	2/4m
				P	PTB210	0.5hPa	2m
				WS/WD	XFY3-1	1m s^{-1}/5°	2/4m
				SDR/SUR	Li200X	5% Max/3% Typical	2/4m
Dome A	80.37°S 77.37°E	4093 m a.s.l.	2005/01- 2020/12	Ta	FS23D	0.05°C	1/2/4m
				RH	HMP35D	2%	4m
				P	6015A	0.5hPa	2m
				WS/WD	12170C/3590B	0.5m s^{-1}/6°	1/2/4m
Kunlun	80.43°S 77.12°E	4093 m a.s.l.	2017/01- 2021/07	Ta	Campbell109/ HMP155	(0.2260- 0028*Ta) °C/1%	2/4m
				RH	HMP155	(0.2260- 0028*Ta) °C/1%	4m
				P	PTB210	0.5hPa	2m
				WS/WD	XFY3-1	1m s^{-1}/5°	4m
				SDR/SUR	Li200X	5% Max/3% Typical	2m
Panda S	82.33°S 75.99°E	4027 m a.s.l.	2008/01- 2021/04	Ta	PRT 2-wire Bridge	0.5°C	4m
				RH	HMP35A	5%	4m
				P	Model 215 A	0.2hPa	4m
				WS/WD	RMYoung/10K Ohmpot	0.2±0.5m s^{-1}/3°	4m

Statement: SDR: downward shortwave radiation; SUR: upward shortwave radiation; LDR: downward longwave radiation; LUR: upward longwave radiation.

https://doi.org/10.5194/essd-2022-188
Preprint. Discussion started: 19 July 2022
© Author(s) 2022. CC BY 4.0 License.

Table 2 The mean values of meteorological variables on AWSs in the PANDA network

Stations\ elements	Air temperature /°C	Relative humidity/%	Pressure /hPa	Wind speed /m s^{-1}
Zhongshan	-10.0	58	985	6.9
Panda 100	-21.6	73	827	11.2
Panda 200	-26.5	72	763	10.9
Panda 300	-30.0	68	726	10.4
Panda 400	-32.0	34	710	10.0
Taishan	-35.4	67	699	10.9
Eagle	-41.2	54	683	3.6
Panda 1100	-47.7	55	603	3.6
Dome A	-50.5	42	575	2.9
Kunlun	-50.8	55	574	3.9
Panda S	-39.2	42	587	4.0